Pollution, 2(4): 475-488, Autumn 2016
DOI: 10.7508/pj.2016.04.009
Print ISSN 2383-451X Online ISSN: 2383-4501
Web Page: https://jpoll.ut.ac.ir, Email: jpoll@ut.ac.ir

Short-term prediction of atmospheric concentrations of ground-level ozone in Karaj using artificial neural network

Asadollahfardi, Gh.*, Tayebi Jebeli, M., Mehdinejad, M. and Rajabipour, M.J.

Department of Civil Engineering, Kharazmi University, Tehran, 43 Mofateh Ave, Iran

Received: 31 May 2016 Accepted: 20 Jun. 2016

ABSTRACT: Air pollution is a challenging issue in some of the large cities in developing countries. Air quality monitoring and interpretation of data are two important factors for air quality management in urban areas. Several methods exist to analyze air quality. Among them, we applied the dynamic neural network (TDNN) and Radial Basis Function (RBF) methods to predict the concentrations of ground-level ozone in Karaj City in Iran. Input data included humidity, hour temperature, wind speed, wind direction, $PM_{2.5}$, PM_{10} and benzene, which were monitored in 2014. The coefficient of determination between the observed and predicted data was 0.955 and 0.999 for the TDNN and RBF, respectively. The Index of Agreement (IA) between the observed and predicted data was 0.921 for TDNN and 0.9998 for RBF. Both methods determined reliable results. However, the RBF neural network performance had better results than the TDNN neural network. The sensitivity analysis related to the TDNN neural network indicated that the $PM_{2.5}$ had the greatest and benzene had the minimum effect on prediction of ground-level ozone concentration in comparison with other parameters in the study area.

Keywords: air pollution, ground-level ozone, Karaj, RBF neural network, TDNN.

INTRODUCTION

Artificial Neural Networks (ANN) are known as one of the artificial intelligence methods, which simply use mathematical models of the human brain as a system. Neural networks are typically trained with data, and they are capable of discovering new connections, new functions or new patterns due to the mentioned features. They have been used widely in various applications, especially in "Air Quality Prediction" in the recent decades, and extensive studies have been carried out on them by researchers. Nowadays, forecasting different parameters of air quality is a major requirement of the environmental and atmospheric managements because of its direct relations with human health. Therefore, the need of accurate models for pollution prediction appears necessary to plan the reduction of air pollution. Air pollution in urban areas is a challenging problem, especially in Karaj City and it causes damaging effects on public health. Reducing air, because of the development of various industries and the increasing number of cars, appears inevitable, and the removal of all sources of pollution or not inserting pollution into the atmosphere seems illogical. Therefore, decreasing air pollution to a safe level so that we make sure that it does not create significant destructive effects is vital. In this case, extensive researches have been conducted on a variety of pollutants such as

* Corresponding author E-mail: asadollahfardi@yahoo.com, Tel: +98 9121192424

prediction of carbon monoxide, nitrogen oxides, ground-level ozone, sulfur oxides, $PM_{2.5}$ and average temperature. Ground-level ozone is one of these pollutants which can lead to serious problems in high concentrations. Industry and worn-out vehicles are the main sources for the production of these pollutants. Chiarelli et al. (2011) explained that the increasing concentration of air pollutants of ozone and particulate matter is leading to an increase in blood pressure over time in Brazil. Gasana et al. (2012) indicated that the children exposed to pollutants of ozone and particulate matter due to motor vehicles in the United States are at risk of asthma more than adults.

Nouri et al. (2008) predicted the average daily monoxide concentrations in Tehran by using multivariate linear regression (MLR) which was based on the principal component and artificial neural network. Their input parameters were PM_{10}, NO_x, SO_2, THC, CH_4, O_3, wind speed, wind direction, temperature, air pressure, humidity and solar radiation. They concluded that a Feed-Forward Multilayer Perceptron (FFMLP) was the best selection for their study.

Noori et al. (2010) predicted daily carbon monoxide concentrations in Tehran using artificial neural network (ANN) and adaptive Neuro- fuzzy inference system (ANFIS). They concluded that the FS– ANN and FS–ANFIS models were the best models considering R^2, mean absolute error and also developed discrepancy ratio statistics. Nejadkoorki and Baroutian (2011) applied ANN to predict PM_{10} concentrations 24-h ahead in Tehran. Yeganeh et al. (2012) predicted daily air pollution in the south of Tehran using a combination of Support Vector Machine (SVM) as a predictor and Partial Least Square (PLS) as a data selection tool based on the measured values of CO concentrations. They concluded that the hybrid PLS–SVM model needed lower computational time than the SVM model as guessed. Noori et al. (2013) applied support vector machine (SVM) to predict CO daily average concentrations. They developed the hybrid model, forward selection (FS)- SVM for CO daily average concentrations forecasting. Azid et al. (2014) applied the combination of principal component (PCA) and artificial neural networks (ANN) to determine its predictive ability for the air pollution index (API). Moazami et al. (2016) indicated that support vector regression (SVR) had less uncertainty in CO prediction than the ANN and adaptive Neuro-fuzzy inference system (ANFIS) models.

Comrie (1997) used the data of eight cities of the United States of Americato identify the ability of artificial neural network model to predict ozone concentrations and his results indicated that the artificial neural network partially presented better results in predicting the daily ozone concentrations. In general, all the studied models partially depend on each region's parameter, and the presence of these parameters affected the results of each developed model. Bonasoni et al. (2000) indicated that vertical profiles of relative humidity and CO and CO_2 gases could be used for the descent of the fullness of ground ozone level. Ribas et al. (2004) investigated the long-term trend of ground-level ozone in several stations with different situations of coast and mountain in urban areas in the Northwest Mediterranean, during an 8-year period and their results revealed that in the coastal stations, the trend of ground-level ozone decreased. Other researchers have applied the ANN method to predict the concentration of ground-level ozone, such as Pastor-Bárcenas et al. (2005) and Hrust et al. (2009). Lu et al. (2006) indicated that using neural network models for the prediction of daily ozone concentrations using parameters such as nitrogen oxide (NO_X), particulate matter (PM_{10}) and sulfur dioxide (SO_2) was more accurate than the estimation of meteorological parameters. Concerning researches in Iran, the study of Seghataleslami et al. (2006) for Mashhad city can be mentioned. In their study, they

applied ANN using hydrocarbon concentrations, nitrogen oxides, air temperature, wind speed, and wind direction as input to the ANN for predicting ground ozone concentrations. Their results indicated that back propagation error algorithm provided solutions with a smaller error percentage compared to the combined algorithm. Paoli et al. (2011) predicted the ground-level ozone concentrations one day in advance by using nitrogen dioxide (NO_2), nitrogen monoxide (NO), sulfur dioxide and particulate matter as input parameters to the ANN for predicting ground ozone concentrations. Reddy et al. (2010) stated that the results of backward trajectory analysis indicating an increase of ozone concentration and the relatively constant high ozone concentrations during the summer might originate from the transport of ozone rich air mass above the boundary layer especially in Northern India and East Asian regions. Sergio et al. (2011) applied principal component to air quality parameters and concluded that the first dataset including NO, NO_X and scalar wind speed had a greater impact on ozone concentrations and the other data set such as temperature and global solar radiation had the most influential parameter. The ANN and support vector machine obtained similar results for ozone prediction. Lu and Wang (2014) applied Multilayer (MLP) and support vector machine (SVM) to predict ground ozone concentrations. They stated that the MLP has the "black-box" property, i.e., it barely provides a physical description for the trained model, over fitting and local minima problems, and SVM has parameters identification and class imbalance problems. Luna et al. (2014) predicted O_3 levels from primary pollutants and meteorological factors, using nonlinear regression methods like ANN and SVM, from primary pollutants and meteorological factors in Rio de Janeiro City. Biancofiore et al. (2015) used a multiple linear regression model and a neural network to predict ozone concentrations. They applied two scenarios, including using meteorological parameters as input to model in the first scenario and the application of both meteorological and photochemical parameters in the second scenario. They concluded that ANN obtains better results.

Study area

Karaj city is located in the west of Tehran province. The area of the city is about 170 km^2. The geographic coordinates are between 35º, 46′ to 35º, 51′ North latitude and 50º, 54′ to 51º, 31′ East longitude. The elevation of Karaj is 1321 m above sea level and the highest point is in the East of Khalajabadi with an altitude of 1,400 m. The lowest point of the city is located in the south of the city at an altitude of 1275 m above sea level. The slope of the city from north to south becomes gentler (Abbaspour Sani et al., 2007). The average humidity is about 51%. The average of maximum relative humidityis 73.1%, and the highest average relative humidity occurs in January. Average of minimum relative humidity of 31.5% is in June which may also reach 17% at a time (Norooz Velashadi et al., 2012). Karaj city has a dry, semi-desert climate in summers and a cold one in winters. The average annual temperature of Karaj is 15 ℃. The minimum temperature is -4 Celsius and the maximum temperature is 40 Celsius (Norooz Velashadi et al., 2012). The Average annual rainfall of Karaj is 252.3 mm. Rainfall in the Northern areas is more than the Southern ones. The month of March with an average of 41.9mm of rain is the rainiest month of the year. Rainfall in winter is 42% (106.2 mm) and then in the spring, 28.9% (73mm), in autumn 26.9% (9.67 mm) and in the summer,2.2% (5.5 mm) (Norooz Velashadi et al., 2012). The average daily wind speed is about 2.2 m/s The prevailing wind direction is from northwest to southeast. Figure 1 indicates the location of the study area. Upper Cambrian silt slates, stone, shale and minor dolomite formations are the oldest geological units of Karaj City.

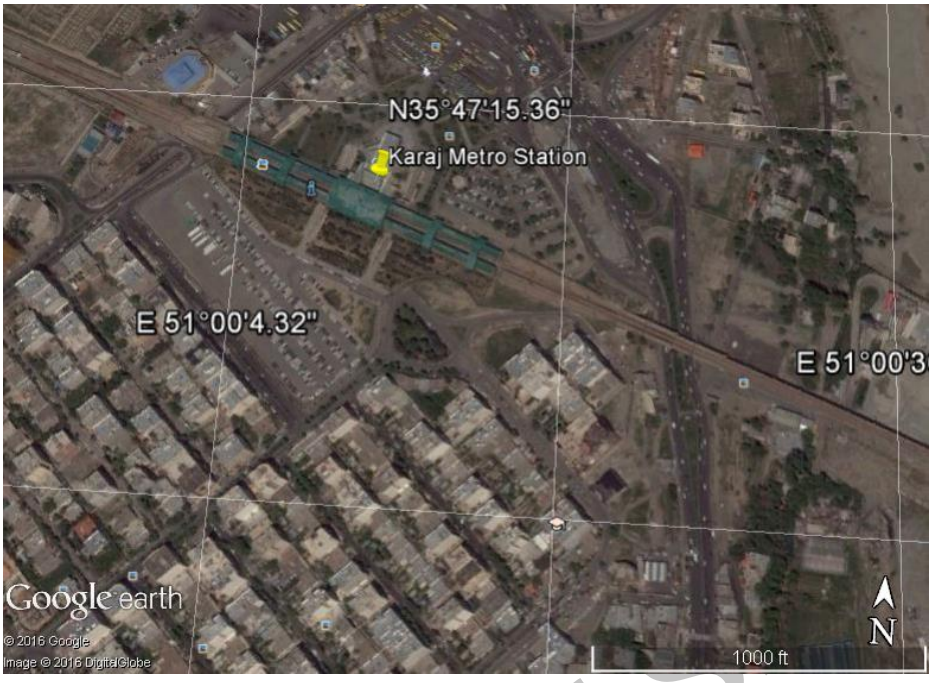

Fig. 1. Location of study area

According to the pollutions of Karaj metropolis and also breathing problems that ground-level ozone causes, especially in the children and the elderly, predicting ground-ozone level for air quality management is vital. We applied the time delay neural network (TDNN) and Radial Basis Function (RBF) neural network to predict concentrations of ground-level ozone. Input data to the models were humidity, hourly temperature, wind speed, wind direction, $PM_{2.5}$, PM_{10} and benzene of the year 2015. The objective of our study was to predict ground-level ozone concentrations in the air of Karaj city by using the TDNN and RBF, and we applied sensitivity analysis to determine which of the input parameters have a great role in predicting ground ozone layer.

We can predict ground level ozone concentrations one day in advance by applying the ANN which may be useful for air quality management. Ozone level concentrations are sensitive to $PM_{2.5}$ which may be beneficial for controlling ground level concentrations to decrease $PM_{2.5}$ in the city.

MATERIALS AND METHODS

The availability or preparation of accurate and sufficient data for the training of the ANN is very important and the power of the ANN for responding to the new problem depends on accurate and sufficient data. Therefore, sufficient and precise data are necessary to train the network well until the network can predict data for the future purposes. In this study, we applied humidity, hourly temperature, wind speed, wind direction, $PM_{2.5}$, PM_{10} and benzene as input to the ANN. The mentioned parameters were hourly recorded. Four hundred and seventy of the data were available, from which 450 were applied for training the network and the rest of them for comparing the simulation data with the observed data. The data were monitored by the Air Quality Control Company (AQCC) of the municipality of Karaj. The AQQC collected data during late January through late March 2014. Table 1 presents a summary statistic of air pollution in Karaj City, which was used in this study.

Table 1. Summary statistics of the data used in this study

$PM_{2.5}$ ($\mu g/m^3$)	Benzene (ppb)	PM_{10} ($\mu g/m^3$)	Wind direction (Degree)	Wind velocity (m/s)	Temperature (C)	Moisture (%)	O_3 (ppb)	Parameter
91	1.13	180	360	13	23	100	64.5	Maximum
1	0.06	4	0	0	-7	11	27.2	Minimum
26.5	0.3	39.6	164.8	3.2	6.93	48.8	38.4	Average
18.02	0.189	22.33	136.16	2.8	6.25	20.8	8.33	Standard deviation
470	470	470	470	470	470	470	470	Count

The ANN is a data processing system, based on a model of the human neurological system that consists of three unique components, including weighting (W), bias (B) and the transfer function (f) (Fig. 2). Output is computed by the Equation (1).

$$a = f\left(n\right) = f\left(WP + b\right) \quad (1)$$

where "p" and "n" are input and output, while "a" is net input and f is transfer function. The input layer works as an interface between the input variable data and the ANN model. Most models also contain one or two hidden layers, although more are possible. These layers implement most of the iterative calculations within the network. The output layer serves as the interface between the ANN model and the end user, transforming model information into an ANN-predicted value of the output variable. Several types of transfer functions exist. Among them, we applied the tangent sigmoid function (Fig. 3), which creates output in the range of (-1, 1) and introduces non-linearity into the network, which can capture non-linear relationships between input and output values (Pastor-Bárcenas et al., 2005).

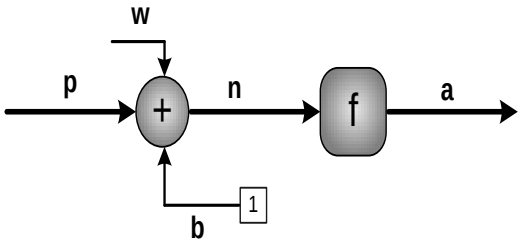

Fig. 2. Schematic of artificial neural network

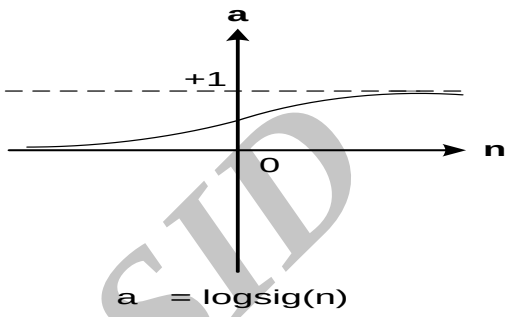

Fig. 3. Transfer function tangent sigmoid

Time delay neural network (TDNN)

The delay operators are introduced to a better understanding of networks TDNN. A delay operator receives the input signal and it has retained a time step closer and the next time step is then output as a result. A Tapped Delay Line (TDL) is created, out of N delay operator series connected. TDL output is vector with N+1 components, including entries of the current time step and N previous time steps (Fig. 4). Network TDNN is created by inclusion of TDLs indifferent layers of a network Multilayer Perceptron (MLP). This network structure is more complex than MLP network. If TDLs would only apply in the input layers, the network would be called "Input Delay Neural Network" (IDNN). The IDNN consists of two main parts: the memory that holds the previous data and the main body which predicts the future events by processing information. The body of this system is usually the static network of MLP, and some TDLs are connected to the input layer. In other words, IDNN is a TDNN whose input layer only has the memory (Fig.5).The IDNN can be modeled by Equations (2) and (3).

$$a_j^1(t) = F\left(\sum_{d=0}^{D}\sum_{i=1}^{R} w_{j,i,d}^1 p_{i,d+1}(t) + b_j^1\right), \quad 1 \le j \le S_1 \tag{2}$$

$$a_k^2(t) = G\left(\sum_{j=1}^{S_1} w_{k,j}^2 a_j^1(t) + b_k^2\right), \ 1 \le k \le S_2 \tag{3}$$

where R is the number of input vector components. S_1 and S_2 are numbers of neural in hidden and output layers, respectively. P is input vector. w^1, w^2 are weighting matrix in hidden and output layers, respectively. b^1, b^2 are bias vectors in hidden and output layers, respectively. G and F are transfer functions in hidden and output layers. α^1, α^2 are output vectors in hidden and output layers, respectively. D is the Degree memory of time delay (Menhaj, 1998). Therefore, this network can be modeled in two parts, the first hidden layers modeling with time delay and modeling the rest of the layers.

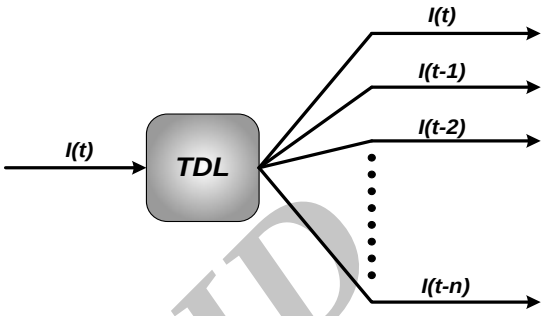

Fig. 4. Tapped delay line

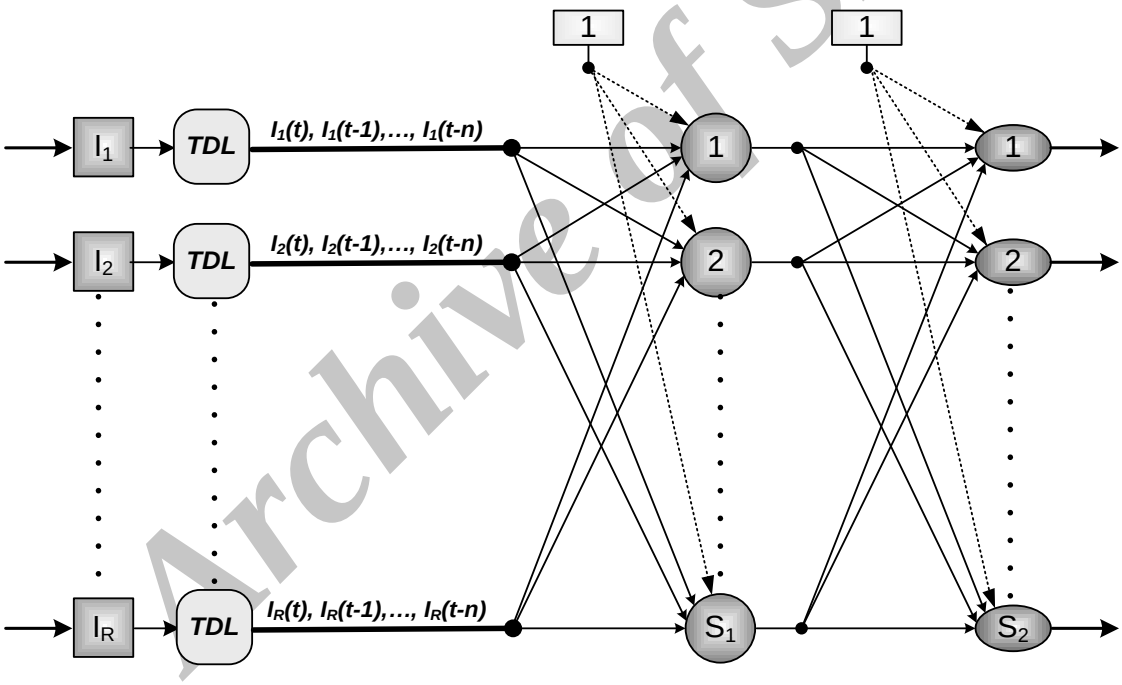

Fig. 5. The IDNN with a hidden layer

Determination of network architecture

- **Separation of nonlinear RBF network**

RBF network is another method for nonlinear separation. The RBF network consists of two fully connected layers, namely, the hidden layer RBF and the output layer (Fig. 6).

Choosing a method of determination of center position is one of the most important sectors in the RBF neural network that will be described below, and this procedure will be performed.

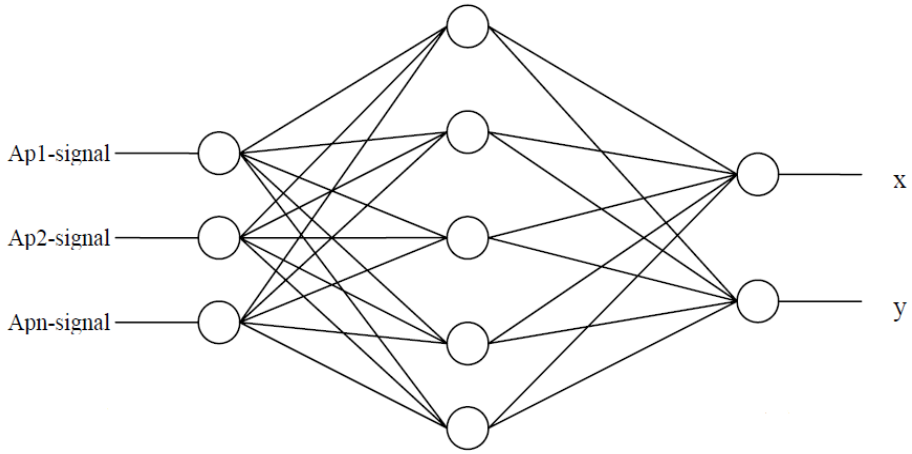

Fig. 6. RBF network with three layers

- **K average algorithm**

In this procedure, K points are randomly selected in space models and then for each of the data learning series, the distance from the K center is calculated and the nearest center is selected for each item of data. Thus comes an initial classification where each data item is assigned to one of the classes of 1 to K, then for all the data, assigned to Class1, the Mean values are attributed to each characteristic. These values, the new center coordinates of class 1 this procedure is repeated for all other classes. Now there are K new centers, distance calculation process of each item of data from the center and their reclassification will be repeated until no change is observed. A total distance of the points of each is measured from the center of the group and the Procedure will not stop until reduction reaches to zero or to its minimum value (Hooti, 2006).

Data preparation

Upon considering using a tangent sigmoid of the transfer function in the hidden layer of the MLP neural network, we changed the scale of the data. All applied data, output and input were transformed to the -1 and 1 interval to prevent network saturation. After finishing the process, the predicted values were transformed back to the real data. We applied Equation (4) to change the scale of the data (Razavi, 2006).

$$As\,(scaled) = \left[\frac{A_i - A}{B - A}\right] \times 2 - 1 \qquad (4)$$

where A_s and A_i are scaled and so are the observed value of the benzene, temperature, humidity and wind speed at time t, respectively. A and B are the lowest and the highest amounts of a series of the parameters. Amounts of weights and biases of the network before starting the education process will have a great impact on the final network response, and it shows the artificial neural networks high sensitivity on initial value parameters. All neural networks used in this study are designed, using the "Neural Network Toolbox" MATLAB software version R2012b.

Evaluation of models

To determine the amount of error in predicting the concentration of ground-level ozone and performance evaluation of the models, we applied Volume Error (VE), Mean Absolute Error (MAE), a Root Mean Squared Error (RMSE) and Mean Bias Error (MBE) which are indicated in Equations (5) through (8) (Neville and Kennedy, 1964).

$$VE = \frac{1}{n}\sum_{t=1}^{n}\left|\frac{O_t - F_t}{O_t}\right| \times 100 \quad (5)$$

$$MAE = \frac{1}{n}\sum_{t=1}^{n}|O_t - F_t| \quad (6)$$

$$RMSE = \sqrt{\frac{1}{n}\sum_{t=1}^{n}(O_t - F_t)^2} \quad (7)$$

$$MBE = \frac{1}{n}\sum_{t=1}^{n}\left|\frac{F_t - O_t}{O_t}\right| \quad (8)$$

where F_t and O_t are the predicted and observed values of ground ozone concentrations at time t, respectively, and n is the number of data. In addition, we applied the Index of Agreement (IA) and coefficient of determination (R^2) between observation and predicted data to illustrate the validity of the model (Equatins 9 and 10; Heckman, 1979).

$$IA = d = 1 - \frac{\sum_{t=1}^{n}(A_t - F_t)^2}{\sum_{t=1}^{n}[(F_t - \bar{A})^2 + (At - \bar{A})]^2} \quad (9)$$

$$R = \frac{\sum(A\_A^{-})\text{^}2}{\sqrt{\sum(A\_A^{-})^2 - \sum(F\_F^{-})^2}} \quad (10)$$

where A_t, F_t and $\bar{A}$ are observed (recorded) data, predicted data and mean observed data, respectively [20]. Where, A and F are observed and predicted data, respectively. $\bar{A}$ and $\bar{F}$ are the average of A and F, respectively (Neville and Kennedy 1964). A high level of R and IA represents a strong correlation between the variables in the two data sets and the low levels of IA and R show poor communication or lack of communication between the two sets (Neville and Kennedy 1964).

- **The RBF neural network**

The RBF neural network has the ability to estimate non-linear relationships. Therefore, it can be used for interpolation issues. A Gaussian RBF is the non-normalized and non-linear form of Gaussian distribution function and has some nice features for incremental learning. Gaussian neural networks are defined to learn complex mappings used to learn, identify and mirror dynamic nonlinear control systems. RBF networks are naturally derived from the interpolated and it is one of the possible solutions to the problem of real multivariate interpolation for data that is non-uniformly sampled. In general, RBF structure is very efficient for the implementation of nonparametric issues and application regression (function approximation). In an RBF network, a Gaussian function is used as a transfer function. We select neuron number of hidden layers equal to the number of input data. The objective of the training process is to reach zero error by increasing epochs. Finally, if the error would not reach zero, the training will stop when the error value, which is obtained during successive epochs, remains constant. RBF neural network with neurons' number equal to the number of input data, is once trained and the error will be found. If this amount is not the net's favorable error, the network is trained again with the number of neurons equal to the number of data, except the weight of each of the neurons, which in this step are modified, and this process is repeated to the end, until the desired response is achieved.

RESULTS AND DISCUSSION

The results of dynamic neural network (TDNN) with a hidden layer

Table 2 indicates some of the neuron results together with their errors in one hidden layer for TDNN network. In this network, a number of different neurons are used to obtain the best result. In this case, from1 to 40 neurons were used in the network, and the network with the number of 32 neurons had the bestresult. This network's MAE, VE, MBE and RMSE were 1.6, 6.2, 0.0604 and 1.060, respectively.

Figure 7 indicates the normal plot of

selecting the proper network. The coefficient of determination between observed and predicted data was 0.955 and the Index of Agreement (IA) was 0.921, which indicates the accuracy of the TDNN model. The horizontal axis of Figure 7 is observed value and the vertical axis is predicted value.

Table 2. The error values for the TDNN network with a hidden layer and different neurons in testing stage.

Neuron number	VE error	MAE error	RMSE error	MBE error
1	42.18	12.62	12.71	0.42
5	40.02	10.65	10.72	0.41
8	44.15	13.56	13.67	0.45
15	41.51	12.32	12.44	0.42
18	38.21	10.02	10.04	0.41
20	36.03	9.6	9.63	0.38
22	24.25	5.12	5.22	0.251
28	12.56	3.42	3.44	0.12
32	6.02	1.6	1.606	0.0604
35	7.87	1.92	1.93	0.078

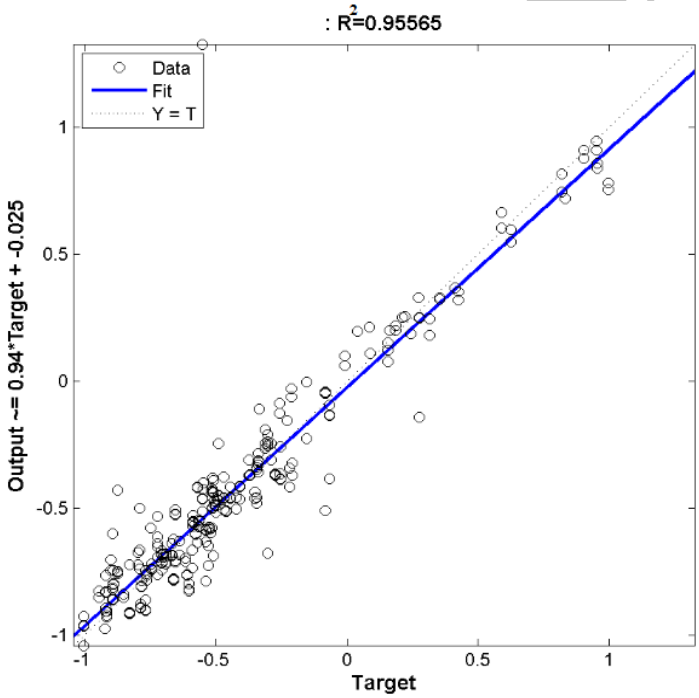

Fig. 7. The normal plot between observed and predicted data in one layer of a TDNN with 32 neurons

As depicted in Figure 8, in the training process of the TDNN network, when iteration numbers (epoch) increase, the Mean Squared Error (MSE) of the network declines. The training step stops in two situations. First, when the number of errors reaches zero. Second, when the numbers of epochs increase and the number of errors does not change. The horizontal axis of Figure 8 is the number of epochs and the vertical axis is MSE. Figure 9 also illustrates a comparison between the observed and the predicted ground-level ozone concentration data. As indicated in Figure 9, relatively good agreement exists between the two types of data.

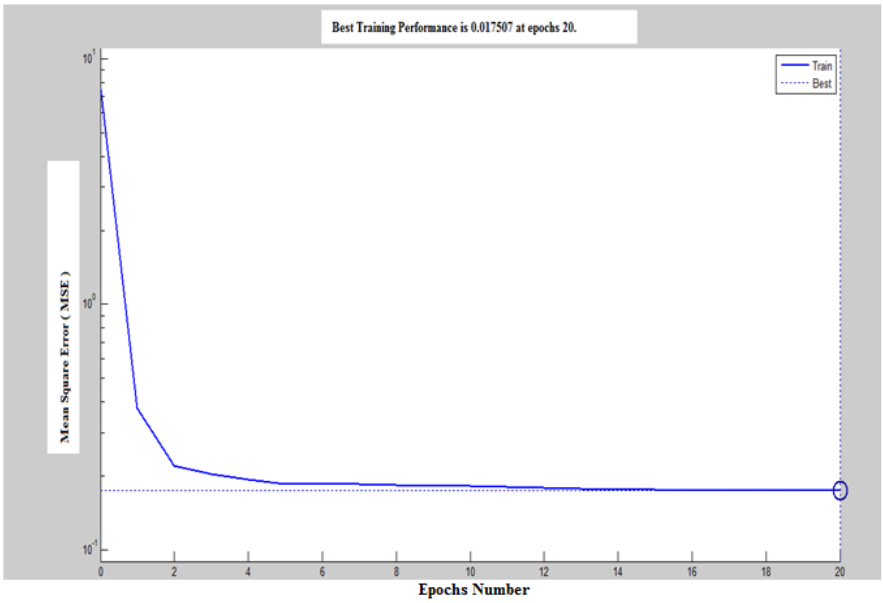

Fig. 8. The performance of the TDNN network in reducing MSE errors in the training process

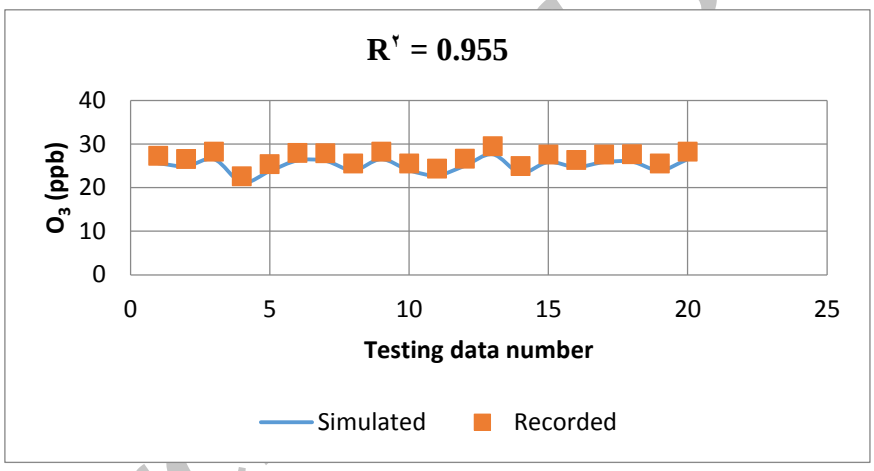

Fig. 9. A comparison between observed and predicted data of the ground-level ozone concentration using the TDNN network

RBF neural network

As indicated in Figure 10, the coefficient of determination between the observed and predicted data was 0.999. Index of agreement (IA) between the observed and predicted data for RBF neural network was 0.921 which indicates a good agreement between the predicted and observed data. Figure 11 indicates the Mean Squared Error (MSE) of the RBF neural network. As illustrated in Figure 11, the MSE decreases as epoch increases. However, after epoch 350 the rate of MSE decrease is higher than before. As indicated in Figure 12, a reasonable agreement between the observed and the simulated data exists in the training process because the coefficient of determination between the observed and predicted data was 0.999. In RBF neural network, the input neurons' number was considered equal to the number of input data and our aim was to reduce the error to zero by increasing epochs. Finally, if the error will not reach zero, the training will be stopped when the error value reaches a constant value. In addition, the VE, MBE and RMSE for RBF neural network were 0.321, 0.0033 and 0.086, respectively.

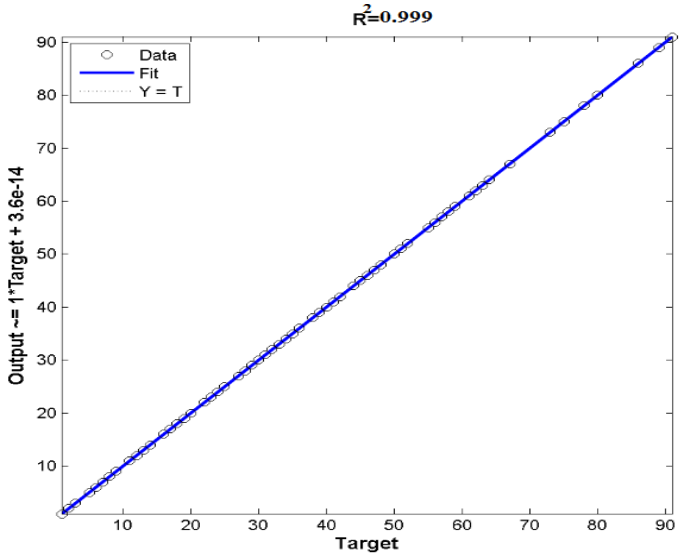

Fig. 10. The coefficient of determination between the observed and predicted data in the RBF neural network for training data

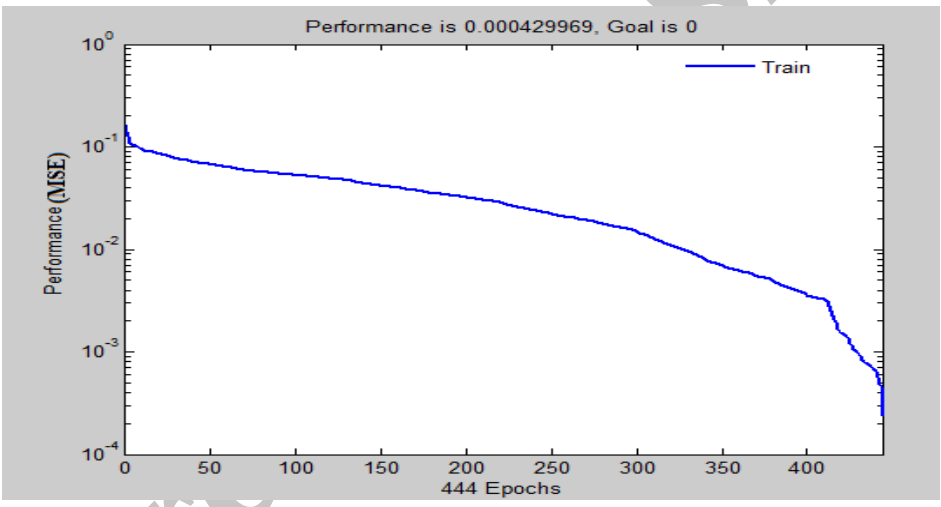

Fig. 11. RBF network performance in reducing the mean squared error

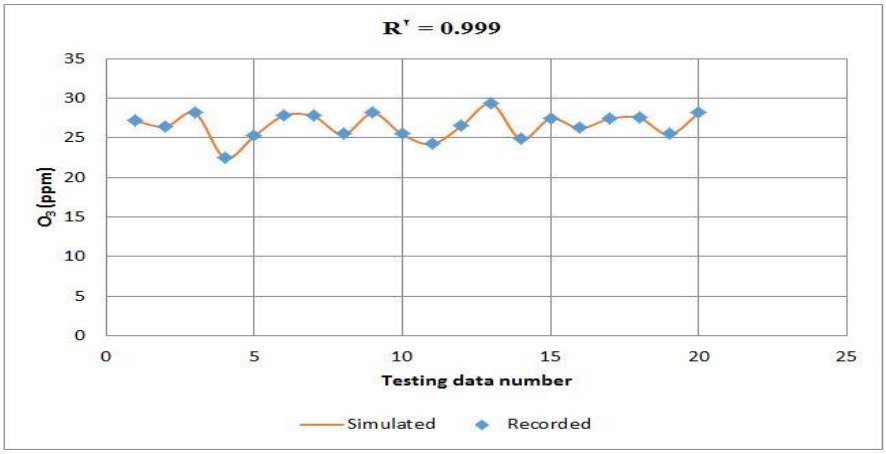

Fig. 12. A comparison between actual results and simulation

Sensitivity analysis

For sensitivity analysis, we increased and decreased 20%, one of the input parameters and the rest of the parameter data remained unchanged. After that, the changed data and other parameter data were used as a new input to the neural network. Afterward, we determined the new coefficient of determination between new predictions and the observed data for ground-level ozone concentration. We continued this procedure for the rest of the parameter data. Table 3 indicates the results of our sensitivity analysis. Figure 13 indicates the results of sensitivity analysis. According to Figure 13, the first factor affecting the prediction of surface ozone concentrations is $PM_{2.5}$; the second factor is wind velocity. The last factor affecting the prediction of ozone concentration is PM_{10}.

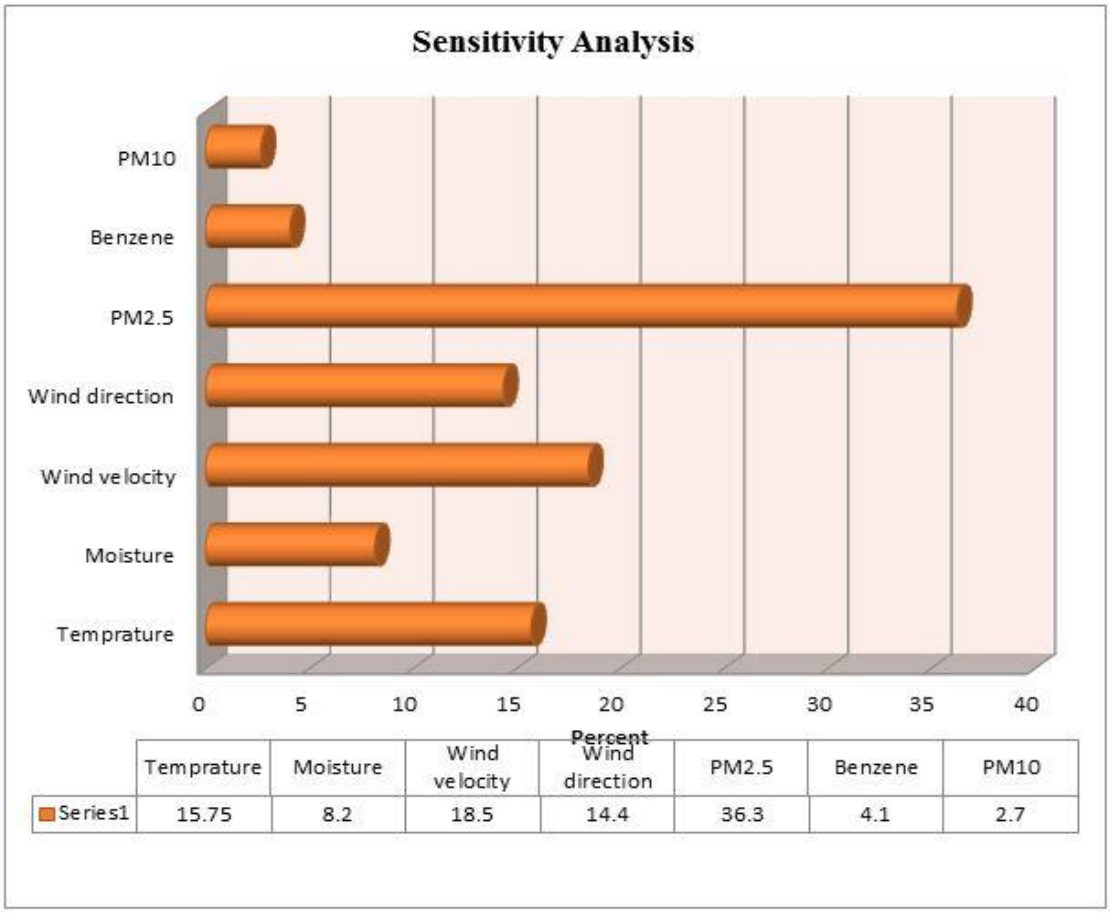

Fig. 13. Comparison of the sensitivity of each parameter in the output

Table 3. The results of the Sensitivity analysis

	R^2		
Parameters	Not changing data	Changing data	Total Errors
Temperature	0.955	0.932	0.023
Wind Velocity	0.955	0.928	0.027
Moisture	0.955	0.943	0.012
Wind direction	0.955	0.934	0.021
$PM_{2.5}$	0.955	0.902	0.053
PM_{10}	0.955	0.951	0.004
Benzene	0.955	0.949	0.006

CONCLUSIONS

In this paper, the applications of neural networks for predicting the concentration of ground-level ozone in the city of Karaj were studied and different results were obtained from our study which are: For TDNN, a hidden layer with 32 neurons reached minimum errors whose VE, MAE, RMSE and MBE were 6.02, 1.6, 1.606 and 0.0604, respectively. The coefficient of determination (R^2) between the observed and predicted ground-level ozone concentration data for both TDNN and RBF neural networks were 0.955 and 0.999, respectively, which indicate the acceptance of the models. The index of agreement (IA) between the observed and predicted ground-level ozone concentration data for both TDNN and RBF neural networks were 0.921 and 0.9998, respectively. The results of sensitivity analysis for TDNN indicated that $PM_{2.5}$ and PM_{10} were the first and the last factors affecting the prediction of surface ozone concentrations. The results of RBF in predicting surface ozone concentrations were more reliable than the results of TDNN. The results of prediction of ground-level ozone prediction may be useful for air quality management in urban area.

REFERENCES

Abbaspour Sani, K.F., Arahmandpour, B. and Hajazi, G. (2007). Determining a base year of sun radiation using 12 year Karaj sun radiation: material and energy research center, a project research.

Azid, A., Juahir, H., Toriman, M.E., Kamarudin, M.K.A., Saudi, A.S.M. CheHasnam, C.N., Abdul Aziz, N.A., Azaman, F., Latif, M.T. et al. (2014). Prediction of the Level of Air Pollution Using Principal Component Analysis and Artificial Neural Network Techniques: a Case study in Malaysia, water ,air &soil pollut., 225(2063), 2-14.

Biancofiore, F., Verdecchia, M., Di Carlo, Tomassetti, B., Aruffo, E., Busilacchio, M., Bianco, S. Di Tommaso, S. and Colangelic, C. (2015). Analysis of surface ozone using a recurrent neural network, Sci.of total environ., 514, 379-3870.

Bonasoni, P., Evangelisti, F., Bonafe, U., Ravegnani, F., Calzolari, F., Stohl, A. and Colombo, T. (2000). Stratospheric ozone intrusion episodes recorded at Mt. Cimone during the VOTALP project: case studies, Atmos. Environ. J., 34 (9), 1355-1365.

Chiarelli, P.S., Pereira, L.A.A., Saldiva, P.H., D.N., Filho, C.F., Garcia, M.L.B., Braga, A.L.F. and Martins, L.C. (2011). The association between air pollution and blood pressure in traffic controllers in Santo André, São Paulo, Brazil, Enviro. Res., 111(5), 650-655.

Comrie, A.C. (1997). Comparing neural networks and regression models for ozone forecasting: J. of the Air & Waste Manag. Associ., 47(6), 653-663.

Gasana, J., Dillikar, D., Mendy, A., Forno, E. and Ramos Vieira, E. (2012). Motor vehicle air pollution and asthma in children: A meta-analysis, Environ. Res., 117, 36-45.

Heckman, J.J. (1979). Sample selection bias as a specification error,Econometrica: J.of the Econom. Soci.,153-161.

Hooti, A. (2006). Assessment of liquefaction potential using artificial neural network: according to cone penetration factor and speed of shear wave, MSc thesis, Khrazmi University.

Hrust, L., Klaić, Z.B., Križan, J., Antonić, O., and Hercog, P. (2009). Neural network forecasting of air pollutant hourly concentrations using optimized temporal averages of meteorological variables and pollutant concentrations: Atmos. Environ. J., 43(35), 5588-5596.

Lu, H.C., Hsieh, J.C. and Chang, T.S. (2006). Prediction of daily maximum ozone concentrations from meteorological conditions using a two-stage neural network: Atmo. Res., 81(2), 124-139.

Luna, A.S., Paredes, M.L.L., de Olivera, G.C.G. and Correa, S.M. (2014). Prediction of ozone concentration in tropospheric levels using artificial neural networks and support vector machine at Rio de Janeiro,Brazil, Atmos. Environ. J., 98, 98-104.

Lu, W.Z. and Wang, D. (2014). learning machine: rational and application in ground-level ozone, App. soft comput., 24,135-141.

Menhaj, M. (1998). Computational Intelligence, Fundamentals ofArtificial Neural Networks. Vol. 1, Amirkabir University publisher (In Persian).

Moazami, S., Noori, R., Jabbarian Amiri, B., Yeganeh, B., Partani, S. and Safavi, S. (2016). Developed support vector machine, Atmos. pollut. Res., 73(3), 412-418.

Neville, A.M., and Kennedy, J.B. (1964). Basic statistical methods for engineers and scientists (International Textbook).

Nejadkoorki, F. and Baroutian, S. (2011).

Forecasting Extreme PM_{10} concentrations using artificial neural network, 6(1), 227-284.

Nouri, R.E., Ashrafi, Kh. and Azhdarpour, A.A.F. (2008). Comparison of ANN and PCA based multivariate regression applied to predict the daily average concentration of carbon monoxide: a case study of Tehran, J. of the earth and space phys., 34(1), 135-152.

Noori, R., Hoshyaripour, G., Afshari, K. and Rasti, O.(2013). Introducing an Appropriate Model using Support Vector Machine for Predicting Carbon Monoxide Daily Concentration in Tehran Atmosphere, Irani. J. Health & Environ, 6(1), 1-10.

Noori, R., Hoshyaripour, G., Ashrafi, K. and Nadjar Araabi, B. (2010). Uncertainty analysis of developed ANN and ANFIS models in prediction of carbon monoxide daily concentration, Atmos. Environ. J., 44(4), 476-482.

Norooz Velashadi, R., Ghahreman, N. and Irannejad, P. (2012). Simulation model to determine humidity and temperature of soil covered by corn plant and soil without covering, Water & Soil J., 26 (1), 55-65.

Paoli, C., Notton, G., Nivet, M.L., Padovani, M. and Savelli, J.L. (2011). A neural network model forecasting for prediction of hourly ozone concentration in Corsica: In Environment and Electrical Engineering (EEEIC), 10th International Conference on (pp. 1-4). May, IEEE.

Pastor-Bárcenas, O., Soria-Olivas, E., Martín-Guerrero, J.D., Camps-Valls, G., Carrasco-Rodríguez, J.L. and Del Valle-Tascón, S. (2005). Unbiased sensitivity analysis and pruning techniques in neural networks for surface ozone modelling: Ecological Modelling, 182 (2), 149-158.

Razavi, F. (2006). Rain Predicting using artificial neural network, M.S thesis. Amir Kabir Univ, Tehran. Iran.

Reddy, B.S.K., Kumar, K.R., Balakrishnaiah, G., Gopal, K.R., Reddy, R.R. Ahammed, Y. N., Lal, S. (2010). Observational studies on the variations in surface ozone concentration at Anantapur in southern India. Atmos.Res., 98 (1), 125-139.

Ribas, A. and Peñuelas, J. (2004).Temporal patterns of surface ozone levels in different habitats of the North Western Mediterranean basin, Atmos. Environ. J., 38, 985-992.

Seghataleslami, N., Mousavi, S.M. and Alami, M. (2006). Modeling and predicting of ozone concentration in air of Mashadusing artificial neural network: ANFIS,11th national conference of Iranian Chem. Eng., Autumn, Iran.

Sergio, C.P., Amador Pereira, L.A., NascimentoSaldiva, P.H.D., Ferreira Filho, C., Bueno Garcia, M.L., Ferreira Braga, A.L. and Conceição Martins, L. (2011). The association between air pollution and blood pressure in traffic controllers in Santo André: São Paulo, Brazil, Environ. Res., 111, 650-655.

Yeganeh, B., Shafie Pour Motlagh, M., Rshidi, Y. and Kamalan, H. (2012) Prediction of CO concentrations based on a hybrid Partial Least Square and Support Vector Machine model, Atmos. Environ. J. 55,357-365.